Mathematical modeling of transmission dynamics and optimal control strategy for COVID-19 in India

M. Ankamma Rao [1] and A.Venkatesh[2*]

[1,2]Department of Mathematics,
AVVM Sri Pushpam College (Affiliated to Bharathidasan University),
Poondi, Thanjavur(Dt), Tamilnadu, India-613 503.

December 28, 2023

Abstract

Mathematical models are being used to investigate the dynamics of disease dissemination, forecast future trends, and access the most effective preventative measures to minimise the extent of epidemic outbreaks. This study formulates an eight compartmental epidemiological model to analyze the COVID-19 dynamics. The stability analysis of infection-free equilibrium is performed. The parameters are estimated by fitting this model to reported confirmed COVID-19 cases in India for 350 days. Sensitivity analysis is executed to identify the most sensitive parameters in this model. An optimal control analysis for India is implemented by incorporating four controls: 1) Public awareness initiatives using the media and civic society to persuade uninfected people not to interact with infected ones, 2) the effort of vaccinating susceptible individuals by supposing all of the susceptible people who got their vaccination are promptly moved to the recovered class 3) encouraging those who are infected with COVID-19 disease to stay at home or join in quarantine centres, as well as encouraging the severe cases admit in the hospital. The results are demonstrated that employing all four control measures significantly reduced the proportion of COVID-19 infections.

Keywords: : Mathematical model, Stability analysis, Sensitivity analysis, optimal control.
Subject Classification: 92D30, 37N25, 34D20, 49J15.

1 Introduction

The most current and dangerous virus is COVID-19, a new coronavirus that initially emerged in early 2020 and is still uncontrolled. Although the first cases are found on 31 December, 2019, in Wuhan, China, the disease's biological origin has not yet been fully determined. Later, the WHO designated the novel coronavirus disease as COVID-19 [1]. On January 30, 2020, the WHO is declared the outbreak a significant global public concern. The COVID-19 pandemic, which is now the major public health issue confronting the world after the Second World War, has already reached 767,972,961 infected cases and more than 6,950,655 fatalities as of July 12, 2023 [2]. Numerous

*Corresponding author: avenkateshmaths@gmail.com

studies demonstrate that COVID-19 may have been a zoonotic (transmitted from animal to human). The significant increase in COVID-19 cases also highlights the crucial fact that secondary dissemination occurs from person to person through direct contact or via particles of the virus dispersed by an infected person's coughing or sneezing.

Mathematical models are used to analyze the dissemination dynamics of epidemic infections with appropriate structures. Among the various models used in the study of epidemic diseases, compartmental models are widely used for the disease dissemination dynamics by subdividing into several compartments based on the need of the investigation [3]. Nowadays researchers prefer the compartmental models for their controllable and simple nature. An overview of several compartmental models is given in [4]. By applying a classical SIR (Susceptible, Infected, Recovered) model to various lockdown situations, Bagal et al. [5] are provided a complete study on COVID-19 spread in lockdown periods. Anand et al [6] are predicted the COVID-19 dissemination in India using the SIR model by considering isolation and testing parameters. This study also analyses the effects of lockdown before and after an rising the COVID-19 cases. At the beginning of the pandemic, the data shown that some infected populations, who has not show any symptoms have capable to spread COVID-19. These individuals are corresponding to the asymptomatic class. The asymptomatic individuals become symptomatic on an average period of three [7]. Similarly, a mathematical model [8] containing 22 compartments was introduced which related to susceptible, exposed, asymptomatic, pre-symptomatic, mildly symptomatic, severely symptomatic, detected, undetected, hospitalized, critical, recovered, dead compartments, etc. These extended models are accurate in defining the process of reality but they could not find perfect values for unknown parameters [9]. In recent years, the researchers are adopted various mathematical modeling approaches using real incidence datasets (especially in the case of COVID-19) with different parameters of the outbreak throughout the world. The concept of optimal control [10], transmissible illnesses must be controlled by giving appropriate dosages at the proper times for preventative measures. In contrast, mathematical modelling of transmissible illnesses has shown that the combination of vaccination, isolation, hospitalisation, and awareness campaigns are required to completely eradicate transmissible illnesses. The implementation of non-pharmaceutical intervention techniques can be a crucial factor in lowering the prevalence of infected populations. Investigating the dissemination of COVID-19 using the theory of optimum control techniques, Silva et al [11] are demonstrated that the diseases require optimal doses to be controlled. Mondal et al [12] are examined the COVID-19 disease dissemination dynamics employing vaccination as a control factor.

Dupey et al. [32] devised an effective computer technique called the Sumudu residual power series method for solving fractional Bloch equations arising in NMR flow. Alshehri et al [33] apply the local fractional natural homotopy perturbation technique to solve specific local fractional partial differential equations with fractal beginning conditions that arise in the physical sciences within the fractal domain. Dupey et al. have constructed a mathematical model for hepatitis E that incorporates a fractional derivative to describe the viral dynamics. Dupey et al. [34] are constructed a model to analyzed using a combination of semi-analytical techniques, including homotopy polynomial equations as well as the Sumudu transform method. Dupey et al.[35] investigated a fractional order model of the phytoplankton-toxic phytoplankton-zooplankton system using the Caputo fractional derivative. They employed three computational methods to investigate this model: the residual power series method, the homotopy perturbation Sumudu transform method, and the homotopy analysis Sumudu transform method. Dupey et al. [36] have created a fractional model that describes the changes in atmospheric CO_2 content. They explored this model using a combination of a semi-analytical homotopy scheme, Sumudu transform, and homotopy polynomials. Devendra et al. [37] devised a hybrid local frac-

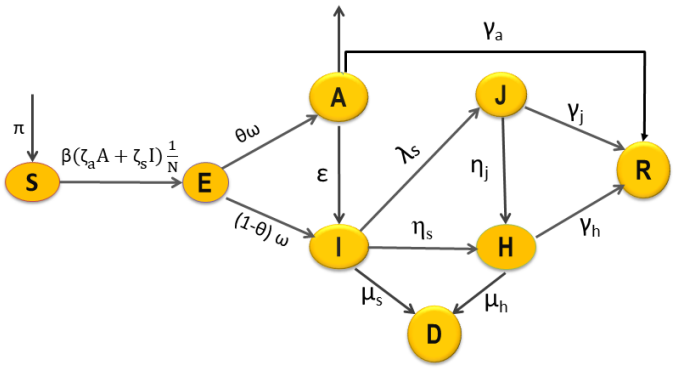

Figure 1: Flow chart of SEAIJHRD model.

tional method for solving certain local fractional partial differential equations. Fractal models can be effectively represented by local fractional derivatives in partial differential equations.

In this study, we are developed a deterministic mathematical model with eight compartments to analyse the COVID-19 dissemination dynamics in India. This model extends to optimal control approach incorporating three distinct control strategies to lower the COVID-19 dissemination. The rest of the article structured as follows: a full explanation of the model formulation is provided in Section.2 The stability analysis of the infection equilibrium is performed and the fundamental reproduction number is determined in Section.3. The model calibration, sensitivity analysis, and effect of parameters on infected classes are performed in Section.4. The optimal control technique with four distinct controls and their numerical simulations are discussed in Section.5. The final section 6 ends with conclusion.

2 Model formulation

In this study we formulate a deterministic mathematical model with eight compartments to analyze the dissemination dynamics of COVID-19. The total population N(t) in this model divided into Susceptible population $(S(t))$, Exposed population $(E(t))$, Asymptomatic infected population (A(t)), Symptomatic infected population $(I(t))$, isolated population $(J(t))$, Hospitalized population $(H(t))$, Recovered population $(R(t))$ and Deceased population $(D(t))$. Then
N (t) = S (t) + E (t) + A (t) + I(t) + J (t) + H (t) + R (t)+D(t).

Dynamics of susceptible population S(t): A susceptible population are those who is at risk of becoming infected by a virus after moving closed with the infected person. This population increased by a constant inflow rate π and diminished by a natural mortality rate μ. In this case $\beta\zeta_a$ and $\beta\zeta_s$ denote the dissemination coefficients of susceptible to asymptomatic and symptomatic populations where ζ_a and ζ_s adjustment factors for

asymptomatic infected and symptomatic infected populations. So the susceptible population decreases at the rates $\beta\zeta_a$ and $\beta\zeta_s$ respectively. The rate of change of susceptible population can be expressed as
$\frac{dS}{dt} = \pi - \beta(\zeta_a A + \zeta_s I)\frac{S}{N} - \mu S.$
Dynamics of exposed population E(t): It is the group of people who have been exposed to COVID-19 but have not yet exhibited any symptoms. As a result of the susceptible individuals exposure to infection, this population grows. At a rate of ω, a portion θ of the exposed population moves to the asymptomatic population (A) and the remaining portion $(1-\theta)$ moves to the symptomatic infected population (I). So the exposed population decreases at rate ω and also it reduces by μ. Hence the rate of change of exposed population is represented as
$\frac{dE}{dt} = \beta(\zeta_a A + \zeta_s I)\frac{S}{N} - (\omega + \mu)E.$
Dynamics of asymptomatic infected population A(t): Asymptomatic infected individuals are those who exposed to the virus but does not shows any symptoms. Since the exposed population transition to the asymptomatic population at the rate ω by a constant proportion θ, this population grows at a portion $\theta\omega$. Since some individuals of the asymptomatic population are recovered themselves at rate γ_a while others become symptomatic at rate ϵ by exhibiting symptoms, this population reduces at rates γ_a and ϵ. This population also diminishes by natural death rate μ. So the rate of change of asymptomatic population is defined by
$\frac{dA}{dt} = \theta\omega E - (\epsilon + \gamma_a + \mu)A.$
Dynamics of symptomatic infected population I(t): Symptomatic infected individuals are those who exposed to COVID-19 virus and are able to spread the disease are considered to be symptomatic. This population grows at the rate $(1-\theta)$ because the constant portion $(1-\theta)\omega$ of exposed population exhibits symptomatic at rate ω. Due to some of this population being isolation at a rate λ_s of and some other population being hospitalised at a rate η_s because of severe illness, this symptomatic population decreases by λ_s and η_s rates. Since some of asymptomatic populations exhibits symptoms at the rate ϵ, the symptomatic individuals decreases at rate ϵ. Also this population diminishes by both symptomatic individuals death rate μ_s and natural death rate μ. As results the rate of change of symptomatic population is stated as
$\frac{dI}{dt} = (1-\theta)\omega E + \epsilon A - (\lambda_s + \eta_s + \mu_s + \mu)I.$
Dynamics of isolated population J(t): Infected population who are join in isolation centers or placed in self-isolation comprise the isolated population. Since some of symptomatic infected individuals are joined in isolation centers at a rate λ_s, this population increases by the rate λ_s. As some of these isolated individuals recovered at a rate γ_j and some are joined in hospitals at the rate η_j due to severe illness, this population decreases at the rates γ_j and η_j. This population also decreases by natural mortality rate μ. So that, the rate of change in the isolated population can be represented by
$\frac{dJ}{dt} = \lambda_s I - (\eta_j + \gamma_j + \mu)J.$
Dynamics of hospitalization population H(t): The hospitalized individuals are those who have developed COVID-19 clinical symptoms and are admitted to the hospital for treatment. Due to severity of illness some of symptomatic infected population and some of isolation population are hospitalized at the rates η_s and η_j. So that this population enhanced by the rates η_s and η_j. Since some of this population recovered at the rate γ_h while other some of this population died at the rate μ_h, this population decreases by the rates γ_h and μ_h.The rate of natural death μ also diminished their population. Hence the rate of change of hospitalized population can be articulated as
$\frac{dH}{dt} = \eta_s I + \eta_j J - (\gamma_h + \mu_h + \mu)H.$
Dynamics of recovered population R(t): These are the individuals who have cured from the asymptomatic infected, isolated, and hospitalized populations. Since some of

the individuals from asymptomatic infected, isolation, and hospitalized populations are recovered from COVID-19 at the rates γ_a, γ_j and γ_h, this population grows by the rates γ_a, γ_j and γ_h. This population also reduces by natural mortality rate μ. Thus the rate of change of recovered population can be represented as
$\frac{dR}{dt} = \gamma_a A + \gamma_j J + \gamma_h H - \mu R$.
Dynamics of deceased population D(t): These are the individuals who died at severeness of COVID-19 disease. This population increases at the mortality rate μ_s of symptomatic infected individuals and at the mortality rate μ_h of hospitalised individuals. Hence the rate of change of deceased population is defined as
$\frac{dD}{dt} = \mu_s I + \mu_h H$.

Using all of the aforementioned biological hypotheses, we provide a graphical depiction of the proposed model in Figure 1 and then the model is governed by the following eight nonlinear system of differential equations as follows :

$$\begin{aligned}
\frac{dS}{dt} &= \pi - \beta(\zeta_a A + \zeta_s I)\frac{S}{N} - \mu S,\\
\frac{dE}{dt} &= \beta(\zeta_a A + \zeta_s I)\frac{S}{N} - (\omega + \mu)E,\\
\frac{dA}{dt} &= \theta\omega E - (\epsilon + \gamma_a + \mu)A,\\
\frac{dI}{dt} &= (1-\theta)\omega E + \epsilon A - (\lambda_s + \eta_s + \mu_s + \mu)I,\\
\frac{dJ}{dt} &= \lambda_s I - (\eta_j + \gamma_j + \mu)J,\\
\frac{dH}{dt} &= \eta_s I + \eta_j J - (\gamma_h + \mu_h + \mu)H,\\
\frac{dR}{dt} &= \gamma_a A + \gamma_j J + \gamma_h H - \mu R,\\
\frac{dD}{dt} &= \mu_s I + \mu_h H.
\end{aligned} \tag{1}$$

with the primary conditions

$$S(0) \geq 0, E(0) \geq 0, A(0) \geq 0, I(0) \geq 0, J(0) \geq 0, H(0) \geq 0, R(0) \geq 0, \& D(0) \geq 0. \tag{2}$$

The information of the various parameters used in the proposed model are listed in Table 1.

3 SEAIJHRD model analysis

3.1 Positivity and boundedness

Theorem 1. *For $t \geq 0$, all the solutions $(S(t), E(t), A(t), I(t), J(t), H(t), R(t), D(t)) \in \boldsymbol{R}^8_+$ of the system (1) with primary conditions (2) are non-negative and uniformly bounded in the specified region Ω.*

Proof. Let $(S(t), E(t), A(t), I(t), J(t), H(t), R(t), D(t)) \in \mathbf{R}^8_+$ be a solution of system (1) for $t \in [0, t_0]$, where $t_0 \geq 0$.
From the first equation of (1), we get
$\frac{dS}{dt} = \pi - (\zeta_a A + \zeta_s I)\frac{S}{N} - \mu S = \pi - \Phi(t)S$, where $\Phi(t) = \beta(\zeta_a A + \zeta_s I)\frac{1}{N} + \mu$.

Table 1: Complete depiction of model parameters of the SEAIJHRD model.

Parameter	Description	Value	Source
π	Net inflow of susceptible population	varies	-
θ	Proportion of exposed population	0.7	[13, 14]
ω	Conversion rate from exposed to infected population	0.4	[14, 15]
ζ_a,	Adjustment factor for asymptomatic infected population	0.3	[16]
ζ_s	Adjustment factor for symptomatic infected population	0.4	[17]
β	Infection dissemination rate	0.5313	Estimated
ϵ	The transition rate of asymptomatic infected individuals to symptomatic infected individuals	0.0168	[18]
λ_s	Isolation rate from symptomatic infected population	0.0828	[19]
η_s	Hospitalization rate of symptomatic infected population	0.0094	Estimated
η_j	Hospitalization rate of isolated population	0.1125	Estimated
γ_a	Recovery rate of asymptomatic population	0.1302	[20]
γ_j	Recovery rate of isolated population	0.017	[21]
γ_h	Recovery rate of hospitalized population	0.07048	[22]
μ_s	Mortality rate of symptomatic infected population	0.00001945	[23]
μ_h	Mortality rate of hospitalization population	0.00001945	[23]
μ	Natural death rate	0.0000391	[24]

Following integration, we obtain
$S(t) = S_0 \exp\left(-\int_0^t \Phi(s)\,ds\right) + \pi \exp\left(-\int_0^t \Phi(s)\,ds\right) \int_0^t e^{\int_0^s \Phi(u)\,du}\,ds > 0.$
From the second equation of (1), we have
$\frac{dE}{dt} = (\zeta_a A + \zeta_s I)\frac{S}{N} - (\omega+\mu)E \geq -(\omega+\mu)E,$
which leads to $E(t) = E_0 \exp(-\int_0^t (\omega+\mu)\,ds) \geq 0$.
The third equation of (1) gives
$\frac{dA}{dt} = \theta\omega E - (\gamma_a + \epsilon + \mu)A \geq -(\gamma_a+\epsilon+\mu)A,$
which implies to $A(t) = A_0 \exp(-\int_0^t (\gamma_a+\epsilon+\mu)\,ds) \geq 0$.
Similarly we can prove that from remaining equations of (1), $I(t) \geq 0$, $J(t) \geq 0$, $H(t) \geq 0$, $R(t) \geq 0$ and $D(t) \geq 0$.
We now establish the system (1) solutions' boundedness.
consider the total population$N = S + E + A + I + J + H + R + D$.
Taking the differentiation of above equation and using (1), we get $\frac{dN}{dt} = \pi - \mu N$,
which leads to $N(t) = N(0)e^{-\mu t} + \frac{\pi}{\mu}(1 - e^{-\mu t})$.
Hence $N(t) \leq \frac{\pi}{\mu}$ if $N(0) \leq \frac{\pi}{\mu}$.
Consequently if $N(0) > \frac{\pi}{\mu}$ then N(t) approaches to $\frac{\pi}{\mu}$ and the amount of infections in E, A, I, J and H shall be zero as $t \to \infty$.
Therefore $S + E + A + I + J + H + R + D \leq \frac{\pi}{\mu}$.
Hence all solution trajectories (S, E, A, I, J, H, R, D) are uniformly bounded in the region $\Omega = \{(S, E, A, I, J, H, R, D) \in \mathbf{R}_+^8 : S + E + A + I + J + H + R + D \leq \frac{\pi}{\mu}\}$. □

3.2 Infection-free equilibrium and fundamental reproduction number

The first seven equations in system (1) are independent of the final equation, so it can be eliminated. By equating the right-hand side of the system of equations (1) to zero and then using $E = A = I = J = H = 0$, the infection-free equilibrium (E^0) of the

model system (1) is obtained. Therefore $E^0 = (\frac{\pi}{\mu}, 0, 0, 0, 0, 0, 0)$.

One of the most important measures in contagious diseases is the fundamental reproduction number R_0. It is defined as the average number of secondary cases that would be generated by a primary infected individual in an entire susceptible population. The total number of infected cases will rise if $R_0 > 1$, as it would at the beginning of an epidemic. Where $R_0 = 1$, the illness is endemic, and if $R_0 < 1$, the total number of cases will decrease. Through the next generation matrix method [25, 26], we determine the fundamental reproduction number R_0 as follows:

$$\mathcal{F} = \begin{pmatrix} \beta\zeta_a + \beta\zeta_s \\ 0 \\ 0 \end{pmatrix} \text{ and } \mathcal{V} = \begin{pmatrix} (\omega+\mu)E \\ -\theta\omega E + (\epsilon+\gamma_a+\mu)A \\ -(1-\theta)\omega E + \epsilon A - (\lambda_s+\eta_s+\mu_s+\mu) \end{pmatrix}$$

The Jacobian matrices of $\mathcal{F}$ and $\mathcal{V}$ at E^0 are expressed as

$$F = \begin{pmatrix} 0 & \beta\zeta_a & \beta\zeta_s \\ 0 & 0 & 0 \\ 0 & 0 & 0 \end{pmatrix} \text{ \& } V = \begin{pmatrix} \omega+\mu & 0 & 0 \\ -\theta\omega & \epsilon+\gamma_a+\mu & 0 \\ -(1-\theta)\omega & -\epsilon & \lambda_s+\eta_s+\mu_s+\mu \end{pmatrix}.$$

The fundamental reproduction number, the largest eigen value of the matrix FV^{-1} is

$$R_0 = \frac{\theta\omega\beta\zeta_a}{(\epsilon+\gamma_a+\mu)(\omega+\mu)} + \frac{\beta\zeta_s[(\epsilon+\gamma_a+\mu)(1-\theta)\omega+\theta\omega\epsilon]}{(\epsilon+\gamma_a+\mu)(\lambda_s+\eta_s+\mu_s+\mu)(\omega+\mu)}$$

Theorem 2. *If $R_0 < 1$ then the infection-free equilibrium $E^0 = (\frac{\pi}{\mu}, 0, 0, 0, 0, 0, 0)$ is locally asymptotically stable (LAS).*

Proof. The variation matrix corresponding to the system (1) at E^0 is
$J_{(E^0)} =$

$$\begin{pmatrix} -\mu & 0 & -\beta\zeta_a & -\beta\zeta_s & 0 & 0 & 0 \\ 0 & \omega+\mu & \beta\zeta_a & \beta\zeta_s & 0 & 0 & 0 \\ 0 & 0 & -(\epsilon+\gamma_a+\mu) & 0 & 0 & 0 & 0 \\ 0 & \theta\omega & \epsilon & -(\lambda_s+\eta_s+\mu_s+\mu) & 0 & 0 & 0 \\ 0 & (1-\theta)\omega & 0 & \lambda_s & -(\eta_j+\gamma_j+\mu) & 0 & 0 \\ 0 & 0 & 0 & \eta_s & \eta_j & -(\gamma_h+\mu_h+\mu) & 0 \\ 0 & 0 & \gamma_a & 0 & \gamma_j & \gamma_h & -\mu \end{pmatrix}$$

The characteristic equation $\mid J_{E^0} - \lambda I \mid = 0$ is represented by
$(\lambda + (\eta_j+\gamma_j+\mu))(\lambda + (\gamma_h+\mu_h+\mu))(\lambda+\mu)^2(\lambda^3 + a_1\lambda^2 + a_2\lambda + a_3) = 0$,
where $a_1 = (\epsilon+\gamma_a+\mu) + (\lambda_s+\eta_s+\mu_s+\mu) + (\omega+\mu)$,
$a_2 = ((\epsilon+\gamma_a+\mu) + (\lambda_s+\eta_s+\mu_s+\mu))(\omega+\mu) + (\epsilon+\gamma_a+\mu)(\lambda_s+\eta_s+\mu_s+\mu) - (\theta\omega\beta\zeta_a + (1-\theta)\omega\beta\zeta_s)$, and
$a_3 = (\epsilon+\gamma_a+\mu)(\lambda_s+\eta_s+\mu_s+\mu)(\omega+\mu)(1-R_0)$.
There are seven eigenvalues, among that the first four values are $-\mu$, -μ, -$(\eta_j+\gamma_j+\mu)$, -$(\gamma_h+\mu_h+\mu)$ and the remaining three eigen values are cube roots of an equation $(\lambda^3 + a_1\lambda^2 + a_2\lambda + a_3) = 0$.
Routh–Hurwitz Criteria asserts that theE^0 is LAS if $a_1 > 0, a_2 > 0, a_3 > 0$ and $a_1a_2 > a_3$.
Clearly $a_1 > 0$ and $a_2 > 0$.
$a_3 = (\epsilon+\gamma_a+\mu)(\lambda_s+\eta_s+\mu_s+\mu)(\omega+\mu)(1-R_0) > 0$ and
$a_1a_2 - a_3 = (\epsilon+\gamma_a+\mu) + (\lambda_s+\eta_s+\mu_s+\mu) + (\omega+\mu)((\epsilon+\gamma_a+\mu) + (\lambda_s+\eta_s+\mu_s+\mu))(\omega+\mu)$
$+ (\epsilon+\gamma_a+\mu)(\lambda_s+\eta_s+\mu_s+\mu) - (\theta\omega\beta\zeta_a + (1-\theta)\omega\beta\zeta_s) - (\epsilon+\gamma_a+\mu)(\lambda_s+\eta_s+\mu_s+\mu)(\omega+\mu)(1-R_0) > 0$ if $R_0 < 1$.
Hence E^0 is LAS if $R_0 < 1$. □

Theorem 3. *The infection free equilibrium* $E^0 = (\frac{\pi}{\mu}, 0, 0, 0, 0, 0, 0)$ *of system* (1) *is globally asymptotic stable (GAS) if* $R_0 < 1$.

Proof. Based on equation (1), it is evident that S and R represent classes that are free from infection, while E, A, I, J, and H represent classes that are infected. Therefore (1) can be expressed as
$\frac{dX}{dt} = U(X, Y)$,
$\frac{dY}{dt} = V(X, Y)$, $V(X, 0) = 0$,
where $X = (S, R) \in \mathbb{R}^2_+$ denotes the disinfected population and $Y = (E, A, I, J, H) \in \mathbb{R}^5_+$ represents the infected population.
Thus $E^0 = (X^*, 0)$ identified as the infection free equilibrium of system (1).
For the model (1), U(X, Y) and V(X, Y) are described as follows:

$$\text{U(X, Y)} = \begin{pmatrix} \pi - \beta(\zeta_a A + \zeta_s I)\frac{S}{N} - \mu S \\ \gamma_a A + \gamma_j J + \gamma_h H - \mu R \end{pmatrix} \text{ \& V(X, Y)} = \begin{pmatrix} \beta(\zeta_a A + \zeta_s I)\frac{S}{N} - (\omega + \mu)E \\ \theta\omega E - (\epsilon + \gamma_a + \mu)A \\ (1-\theta)\omega E + \epsilon A - (\lambda_s + \eta_s + \mu_s + \mu)I \\ \lambda_s I - (\eta_j + \gamma_j + \mu)J \\ \eta_s I + \eta_j J - (\gamma_h + \mu_h + \mu)H \end{pmatrix}$$

From the expression V(X, Y), easily show that V(X, 0) = 0
To prove that E^0 is GAS, we verify the following two conditions
(I). $\frac{dX}{dt} = U(X, 0)$ where X^* is GAS.
(II). $V(X, Y) = KY - \bar{V}(X, Y)$, $\bar{V}(X, Y) \geq 0$, for $(X, Y) \in \Omega$
where $K = D_Y V(X^*, 0)$ is M- Matrix in the region Ω.
The deterministic model system (1) stated in (I) can be expressed as

$\frac{d}{dt}\begin{pmatrix} S \\ R \end{pmatrix} = \begin{pmatrix} \pi - \mu S \\ -\mu R \end{pmatrix}$,
$\Rightarrow S(t) = \frac{\pi}{\mu} + (S(0) - \frac{\pi}{\mu})e^{-\mu t}$ and $R(t) = R(0)e^{-\mu t}$

As $t \to \infty$, $S(t) = \frac{\pi}{\mu}$ and $R(0) = 0$.

Thus X^* is GAS for $\frac{dX}{dt} = U(X, 0)$ and hence the first condition (I) is satisfied for system (1).

Now the matrices K and $\bar{V}(X, Y)$ of model system (1) can be expressed as K =

$$\begin{pmatrix} -(\omega+\mu) & \beta\zeta_a & \beta\zeta_s & 0 & 0 \\ \theta\omega & -(\epsilon+\gamma_a+\mu_a+\mu) & 0 & 0 & 0 \\ (1-\theta)\omega & \epsilon & -(\lambda_s+\eta_s+\mu_s+\mu) & 0 & 0 \\ 0 & 0 & \lambda_s & -(\eta_j+\gamma_j+\mu) & 0 \\ 0 & 0 & \eta_s & \eta_j & -(\gamma_h+\mu_h+\mu) \end{pmatrix}$$

$$\text{\& } \bar{V}(X, Y) = \begin{pmatrix} \beta(\zeta_a A(1-\frac{S}{N}) + \zeta_s I(1-\frac{S}{N}) \\ 0 \\ 0 \\ 0 \\ 0 \end{pmatrix}.$$

Since all non-diagonal elements of matrix K are non-negative, K is M- matrix and as $S(t) \leq N(t)$, $\bar{V}(X, Y) \geq 0$ for all $(X, Y) \in \Omega$.
Thus the (II) condition is satisfied.
Hence E^0 is GAS for $R_0 < 1$. □

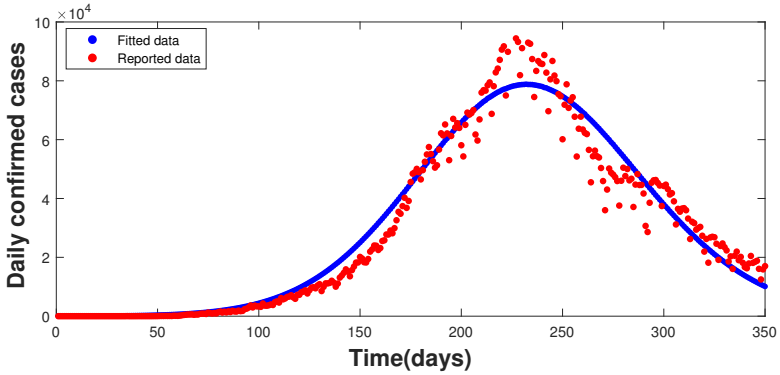

Figure 2: Model fitting based on reported data.

4 Numerical simulation

4.1 Model calibration

In this section, the model (1) fits to confirmed COVID -19 cases for all over India acquired from official site COVID-19 India API (Application Programming Interface) [27] in time period between January 30, 2020, and January 12, 2021. The parameter values β, η_s and η_j are estimated by minimizing the sum of squared error (SSE) method (lsqnonlin function) in MATLAB. We minimize the sum of squared error (SSE) as $SSE = \sum_{t=1}^{n}((Z(t) - \bar{Z(t)})^2$.
where $Z(t)$ denotes the reported COVID-19 confirmed cases while $\bar{Z(t)}$ signifies the model (1) output respectively. The estimated parameter values and other fixed parameter values obtained from the literature are listed in Table 1. Figure 2 illustrates that the model fit with the daily COVID-19 confirmed cases in India. The model solution is represented by red circles, while the reported data is shown by a blue dotted line.

4.2 Sensitivity analysis

Sensitivity analysis performance is very important in detecting the influence of different parameters in the spreading of the coronavirus. This method is very useful for discerning the increase and decrease in the R_0 value with respect to different parameters. A complete report of dengue fever sensitivity is executed in [28]. The sensitivity of parameters defines whether the contagious diseases will spread throughout the population or not. Through sensitive analysis, we analyze the influence of parameters on the model. Whenever parameters are determined, different techniques can be carried out for attaining excellent results. Through the normalized forward sensitivity technique [29] a for R_0, normalized forward sensitivity index of significant parameter p is determined as $\Gamma_p^{R_0} = \frac{\partial R_0}{\partial p} \times \frac{p}{R_0}$.

The parameter on R_0 that has a greater magnitude index is more sensitive. If the sensitivity index is positive, R_0 grows as the parameter p grows. Similarly if the sensitivity index has a negative sign, in which case R_0 falls as p grows. Thus, our sensitivity analysis yields the parameters ζ_a, ζ_s, ω and β have positive effect on R_0 while the parameters θ, λ_s, η_s, γ_a, μ_s and μ are the negative effect on R_0. Among these parameters ζ_a, ω and β are more effective on rise of R_0 whereas λ_s and η_s are more efficient on fall of R_0.

Figure 4(a) indicates the contour Plot of R_0 in relation to virus dissemination rate

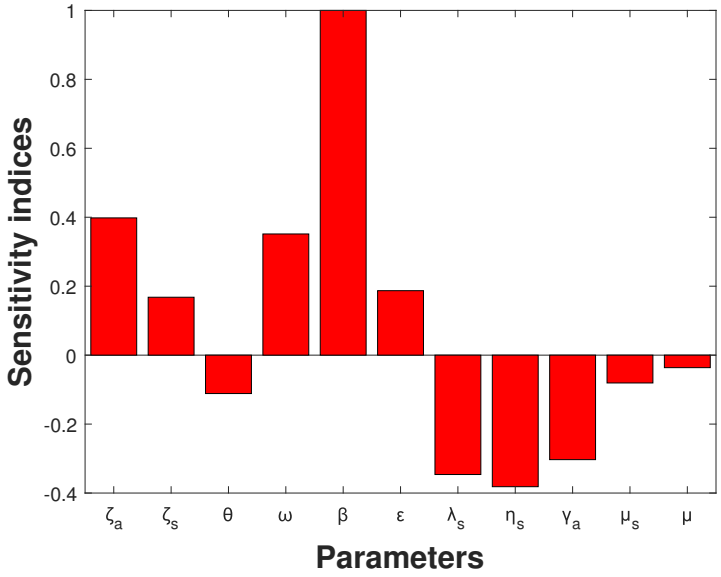

Figure 3: Sensitivity indices of R_0

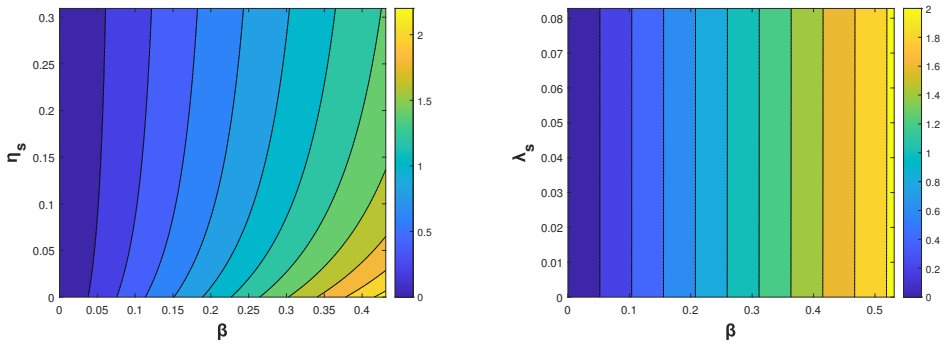

(a) (b)

Figure 4: Contour plots of R_0 with respect to parameters (a)(β, η_s) and (b)(β, λ_s).

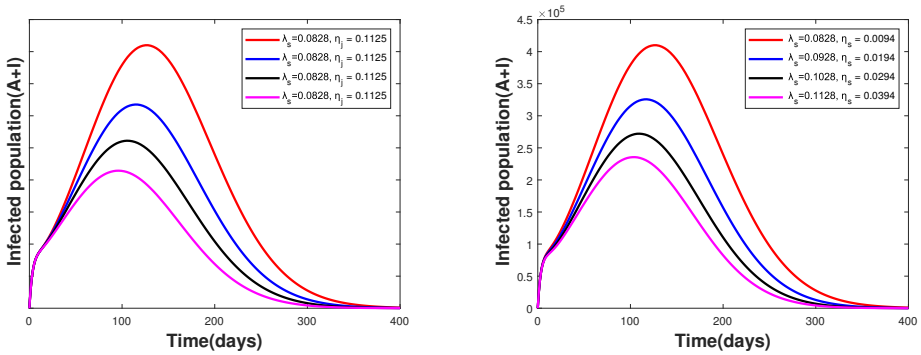

(a) (b)

Figure 5: Variations in infected population with respect to parameters (a) (λ_s, η_j) and (b) (λ_s, η_s).

(β) and hospitalization rate (η_s) from symptomatic infected population. This plot is revealed that whenever the contact rate(β) decreases and the hospitalization rate(η_s) increases, the basic reproduction number decreases. Figure 4(b) indicates the contour Plot of R_0 in relation to virus dissemination rate (β) and quarantine rate (λ_s) from symptomatic infected populations. This plot is demonstrated that whenever the contact rate (β) decreases and quarantine rate (λ_s) increases, the R_0 value decreases so that the spreading of virus decreases.

4.3 COVID-19 Prevalence changes with significant parameters

In this section, we analyse the effect of parameters on infected population. Figure 5 is demonstrated that the infected population reduces when the isolation rate (λ_s) of symptomatic infected population and hospitalization rate (η_j) of isolated population risen. Similarly the disease dissemination will be decreased if both isolation and hospitalization rates of symptomatic infected population increased.

5 Optimal control

5.1 Optimal control model

In the fields of engineering, sciences, and economics, optimal control has major significance. Optimal control is used in detecting parameters that can control definite variables to yield the optimum result. By implementing the most effective intervention measures, we aim to reduce the number of infected, isolated, and hospitalised individuals. The system (1) is extended to optimal control model by including four control variables u, v, w_1 and w_2. The control u involves awareness campaigns in the media and in civil society to encourage people to use face masks, sanitation and keep their distance from infected people to diminish the spread of disease. The second control v represents the effort of vaccinating susceptible individuals by supposing all of the susceptible people who got their vaccination are promptly moved to the recovered class. The last two controls w_1 and w_2 represent encouraging the asymptomatic infected individuals to join isolation and symptomatic infected individuals to join either hospitals or isolated. As a result, w_1 and w_2 are evaluated in comparison to improved medical facilities, such as an increase

in beds, ventilators, mobile isolation centres, etc. Therefore the set of four controls is defined as

$$\mathcal{U} = \{u, v, w_1, w_2 : \text{Lebesgue integral and} \quad 0 \leq u, v, w_1, w_2 \leq 1, \quad t \in [0, T]\}.$$

Taking into account all of the aforementioned presumptions, the formulated optimal control model is

$$\begin{aligned}
\frac{dS}{dt} &= \pi - (1-u(t))\beta(\zeta_a A + \zeta_s I)\frac{S}{N} - \mu S - v(t)S, \\
\frac{dE}{dt} &= (1-u(t))\beta(\zeta_a A + \zeta_s I)\frac{S}{N} - (\omega + \mu)E, \\
\frac{dA}{dt} &= \theta\omega E - (\epsilon + \gamma_a + \mu)A - w_1(t)A, \\
\frac{dI}{dt} &= (1-\theta)\omega E + \epsilon A - (\lambda_s + \eta_s + \mu_s + \mu)I - w_2(t)I, \\
\frac{dJ}{dt} &= w_1(t)A + \lambda_s I - (\eta_j + \gamma_j + \mu)J + \rho w_2(t)I, \\
\frac{dH}{dt} &= \eta_s I + \eta_j J - (\gamma_h + \mu_h + \mu)H + (1-\rho)w_2(t)I, \\
\frac{dR}{dt} &= \gamma_a A + \gamma_j J + \gamma_h H - \mu R + v(t)S, \\
\frac{dD}{dt} &= \mu_s I + \mu_h H.
\end{aligned} \tag{3}$$

For the fixed T, the objective functional is presented by

$$\mathcal{J} = \int_0^T (C_1 A + C_2 I + C_3 J + C_4 H + \frac{1}{2}(C_5 u^2 + C_6 v^2 + C_7 w_1^2 + C_8 w_2^2)\ dt. \tag{4}$$

Here C_1, C_2, C_3, C_4, C_5, C_6, C_7 and C_8 are non negative weight constants.

The objective is to determine the control variables u^*, v^*, w_1^* and w_2^* such that $\mathcal{J}(u^*, v^*, w_1^*, w_2^*) = \min_{u,v,w_1,w_2 \in \mathcal{U}} \mathcal{J}(u, v, w_1, w_2)$.
The Lagrangian of this model (3) is
$\mathcal{L}(S, E, A, I, J, H, R, D, u(t), v(t), w_1(t), w_2(t)) = C_1 A + C_2 I + C_3 J + C_4 H + \frac{1}{2}(C_5 u^2 + C_6 v^2 + C_7 w_1^2 + C_8 w_2^2)$.
For this problem, the Hamiltonian function $\mathcal{H}$ is defined as
$\mathcal{H} = C_1 A + C_2 I + C_3 J + C_4 H + \frac{1}{2}(C_5 u^2 + C_6 v^2 + C_7 w_1^2 + C_8 w_2^2) + \lambda_1 \frac{dS}{dt} + \lambda_2 \frac{dE}{dt} + \lambda_3 \frac{dA}{dt} + \lambda_4 \frac{dI}{dt} + \lambda_5 \frac{dJ}{dt} + \lambda_6 \frac{dH}{dt} + \lambda_7 \frac{dR}{dt} + \lambda_8 \frac{dD}{dt}$.
where λ_i for i = 1,2,3,...8 are the adjoint variables.

Theorem 4. *If the couple (S^*, E^*, A^*, I^*, J^*, H^*, R^*, D^*) is solutions of the system* (3) *that minimizes the objective functional* (4) *with relation to optimal controls $u^*(t)$, $v^*(t)$, w_1^*, $w_2^* \in \mathcal{U}$, then there are adjoint variables λ_i for i =1,2,3,...8 satisfies the*

canonical equations:

$$\begin{aligned}
\lambda_1' &= -\frac{\partial \mathcal{H}}{\partial S} = (\lambda_1-\lambda_2)\beta(1-u)(\zeta_a A+\zeta_s I)\frac{1}{N}+(\lambda_1-\lambda_7)v+\lambda_1\mu,\\
\lambda_2' &= -\frac{\partial \mathcal{H}}{\partial E} = (\lambda_2-\lambda_4)\omega+(\lambda_4-\lambda_3)\theta\omega+\lambda_2\mu,\\
\lambda_3' &= -\frac{\partial \mathcal{H}}{\partial A} = -C_1+(\lambda_1-\lambda_2)\beta(1-u)\frac{\zeta_a S}{N}+(\lambda_3-\lambda_4)\epsilon+(\lambda_3-\lambda_5)w_1+(\lambda_3-\lambda_7)\gamma_a+\lambda_3\mu,\\
\lambda_4' &= -\frac{\partial \mathcal{H}}{\partial I} = -C_2+(\lambda_1-\lambda_2)\beta(1-u)\frac{\zeta_s S}{N}+(\lambda_4-\lambda_5)\lambda_s+(\lambda_4-\lambda_6)(\eta_s+w_2)\\
&\quad +(\lambda_6-\lambda_5)\rho w_2+(\lambda_4-\lambda_7)\mu_s+\lambda_4\mu,\\
\lambda_5' &= -\frac{\partial \mathcal{H}}{\partial J} = -C_3+(\lambda_5-\lambda_6)\eta_j+(\lambda_5-\lambda_7)\gamma_j+\mu\lambda_5,\\
\lambda_6' &= -\frac{\partial \mathcal{H}}{\partial H} = -C_4+(\lambda_6-\lambda_7)\gamma_h+(\lambda_6-\lambda_8)\mu_h+\mu\lambda_6,\\
\lambda_7' &= -\frac{\partial \mathcal{H}}{\partial R} = \mu\lambda_7,\\
\lambda_8' &= -\frac{\partial \mathcal{H}}{\partial D} = 0.
\end{aligned}$$

with the transversality conditions at time T: $\lambda_i(T)=0$*, for all i=1,2,3,...,8. Furthermore the corresponding optimal controls* $u^*(t)$*,* $v^*(t)$*,* $w_1^*(t)$ *and* $w_2^*(t)$ *are given by*
$u^*(t)=\min\{1,\max(0,\frac{1}{NC_5}(\lambda_1-\lambda_2)\beta S(\zeta_a A+\zeta_s I))\}$,
$v^*(t)=\min\{1,\max(0,\frac{1}{C_6}((\lambda_1-\lambda_7)S))\}$,
$w_1^*(t)=\min\{1,\max(0,\frac{1}{C_7}((\lambda_3-\lambda_5)A))\}$, *and*
$w_2^*(t)=\min\{1,\max(0,\frac{1}{C_8}((\lambda_4-\lambda_6)+\rho(\lambda_6-\lambda_5))I)\}$.

Proof. We examine the necessary criteria for the control variables using the maximum principle of Pontryagin for the system (3). To achieve this, for all $t\in[0,T]$, we define the Hamiltonian $\mathcal{H}$ as

$\mathcal{H} = C_1A+C_2I+C_3J+C_4H+\frac{1}{2}(C_5u^2+C_6v^2+C_7w_1^2+C_8w_2^2)+\lambda_1(\pi-(1-u(t))\beta(\zeta_aA+\zeta_sI)\frac{S}{N}-\mu S-v(t)S)+\lambda_2((1-u(t))\beta(\zeta_aA+\zeta_sI)\frac{S}{N}-(\omega+\mu)E)+\lambda_3(\theta\omega E-(\epsilon+\gamma_a+\mu)A-w_1(t)A)+\lambda_4((1-\theta)\omega E+\epsilon A-(\lambda_s+\eta_s+\mu_s+\mu)I-w_2(t)I)+\lambda_5(w_1(t)A+\lambda_sI-(\eta_j+\gamma_j+\mu)J+\rho w_2(t)I)+\lambda_6(\eta_sI+\eta_jJ-(\gamma_h+\mu_h+\mu)H+(1-\rho)w_2(t)I)+\lambda_7(\gamma_aA+\gamma_jJ+\gamma_hH-\mu R+v(t)S)+\lambda_8(\mu_sI+\mu_hH)$.
Because of maximum principle of Pontryagin [30], there are co-states λ_1', λ_2', λ_3',...,λ_8' that satisfying the following canonical equations
$\lambda_1'=-\frac{\partial\mathcal{H}}{\partial S}$, $\lambda_2'=-\frac{\partial\mathcal{H}}{\partial E}$, $\lambda_3'=-\frac{\partial\mathcal{H}}{\partial A}$, $\lambda_4'=-\frac{\partial\mathcal{H}}{\partial I}$,...,+ $\lambda_8'=-\frac{\partial\mathcal{H}}{\partial D}$.
with transversality conditions $\lambda_i(T)=0$, for all i=1,2,3,...,8.
Now we get the optimal controls by using the optimal condition, $\frac{\partial\mathcal{H}}{\partial u}=0$, $\frac{\partial\mathcal{H}}{\partial v}=0$, $\frac{\partial\mathcal{H}}{\partial w_1}=0$ and $\frac{\partial\mathcal{H}}{\partial w_2}=0$.
$\frac{\partial\mathcal{H}}{\partial u}=C_5u+\beta\lambda_1(\zeta_aA+\zeta_sI)\frac{S}{N}-\lambda_2(\zeta_aA+\zeta_sI)\frac{S}{N}=0$.
Then $u=\frac{\beta S(\zeta_aA+\zeta_sI)}{NC_5}(\lambda_1-\lambda_2)$ at $u=u^*$.
$\frac{\partial\mathcal{H}}{\partial v}=C_6v-\lambda_1S+\lambda_7)S=0$.
Then $v=\frac{1}{C_6}(\lambda_1-\lambda_7)S$ at $v=v^*$.
$\frac{\partial\mathcal{H}}{\partial w_1}=C_7w_1-\lambda_3A+\lambda_5A=0$.
Then $w_1=\frac{1}{C_7}(\lambda_3-\lambda_5)A$ at $w_1=w_1^*$.
$\frac{\partial\mathcal{H}}{\partial w_2}=C_8w_2-(\lambda_4-\lambda_6)I-(\lambda_5-\lambda_6)\rho I=0$.
Then $w_2=\frac{1}{C_8}((\lambda_4-\lambda_6)+\rho(\lambda_6-\lambda_5))I$ at $w_1=w_2^*$.
By taking the bounds for u(t), v(t), $w_1(t)$ and $w_2(t)$, we characterize the optimal controls:

$u^*(t) = \min\{1, \max(0, \frac{1}{NC_5}(\lambda_1 - \lambda_2)\beta S(\zeta_a A + \zeta_s I))\}$,
$v^*(t) = \min\{1, \max(0, \frac{1}{C_6}((\lambda_1 - \lambda_7)S))\}$,
$w_1^*(t) = \min\{1, \max(0, \frac{1}{C_7}((\lambda_3 - \lambda_5)A))\}$ and
$w_2^*(t) = \min\{1, \max(0, \frac{1}{C_8}((\lambda_4 - \lambda_6) + \rho(\lambda_6 - \lambda_5))I)\}$. □

5.2 Optimal control model simulation

The model simulation is carried out in MATLAB during the time interval [0,400] using the model parameters listed in Table 1. The optimality system is solved by an iterative method. The extended system (3) is computed by using forward difference approximation [31] and then the adjoint system is calculated by using backward difference approximation. Choose $C_1 = 1$, $C_2 = 1$, $C_3 = 1$, $C_4 = 1$, $C_5 = 40$, $C_6 = 50$, $C_7 = 55$ and $C_8 = 55$ with the initial conditions $S(0) = 1217378052, E(0) = 13000, A(0) = 5, I(0) = 2, J(0) = 1, H(0) = 1$, $R(0) = 0$ and $D(0) = 0$. Figure 6 displays that variations in susceptible, exposed, asymptomatic infected, symptomatic infected, isolated, hospitalized, recovered and deceased populations within and without controls. This Figure is illustrated that the infected populations with controls swiftly decreased in comparison to the populations without controls, whereas the disinfected populations with controls rapidly increased in comparison to the disinfected population without controls. The optimal control variable profiles of u(t), v(t), $w_1(t)$ and $w_2(t)$ are shown in Figure 7. From this Figure, it can be observed that, in comparison to $w_1(t)$ and $w_2(t)$ controls, the controls u(t) and v(t) which related to awareness campaigns and vaccinating of susceptible population must be kept at 1 over a longer period of time. Figure 8 illustrates the variations in control profile related cost for each control increases. This Figure is demonstrated that the time needed to maintain these controls at 1 decreases if the cost of each control variables is risen.

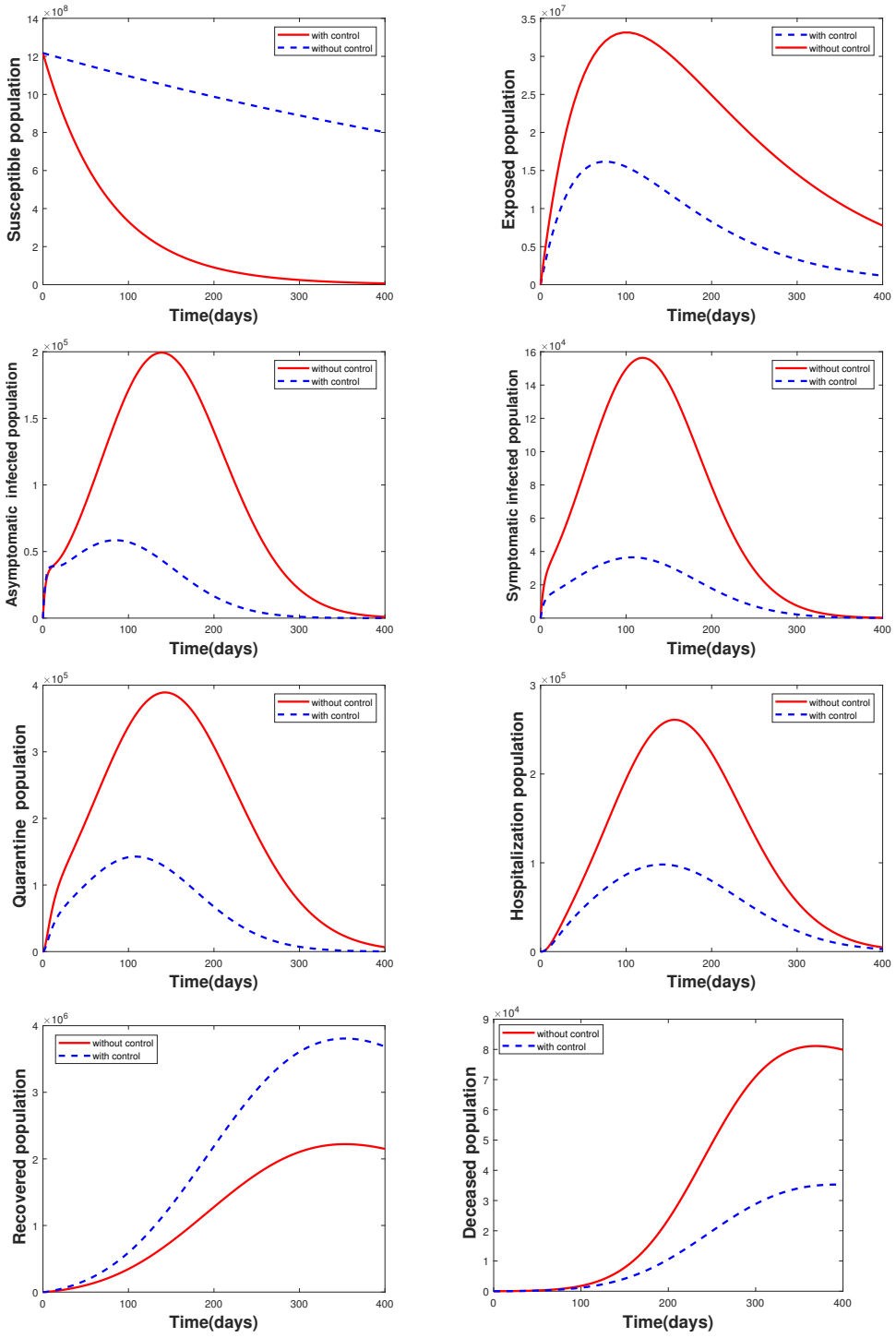

Figure 6: Variations in infected and disinfected populations with and without controls.

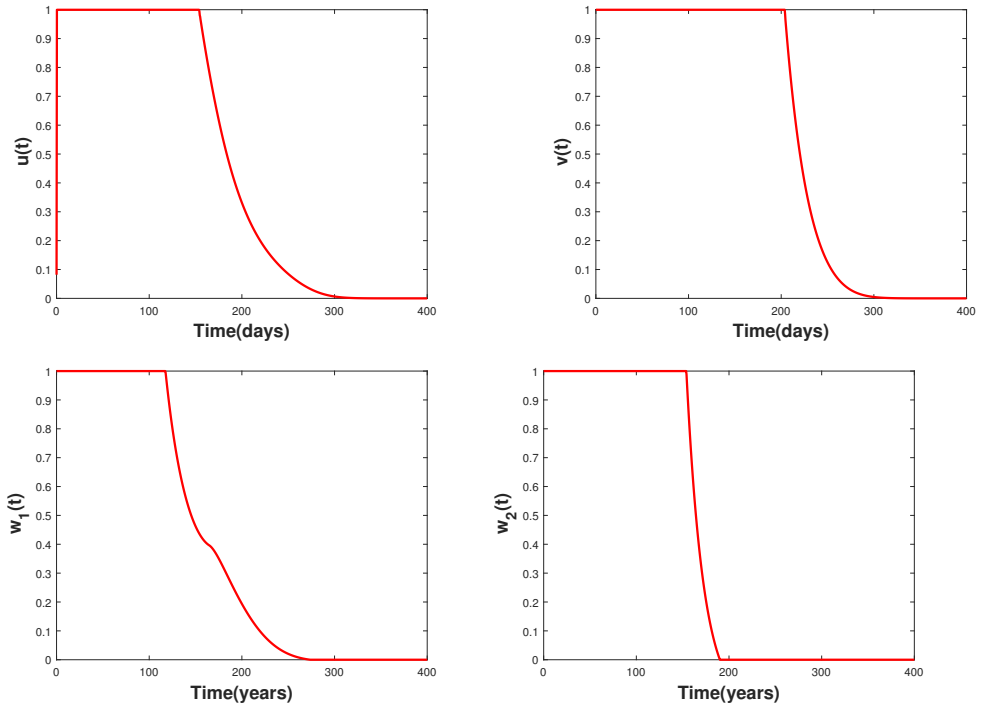

Figure 7: Optimal control variable profiles u(t), v(t), $w_1(t)$ and $w_2(t)$.

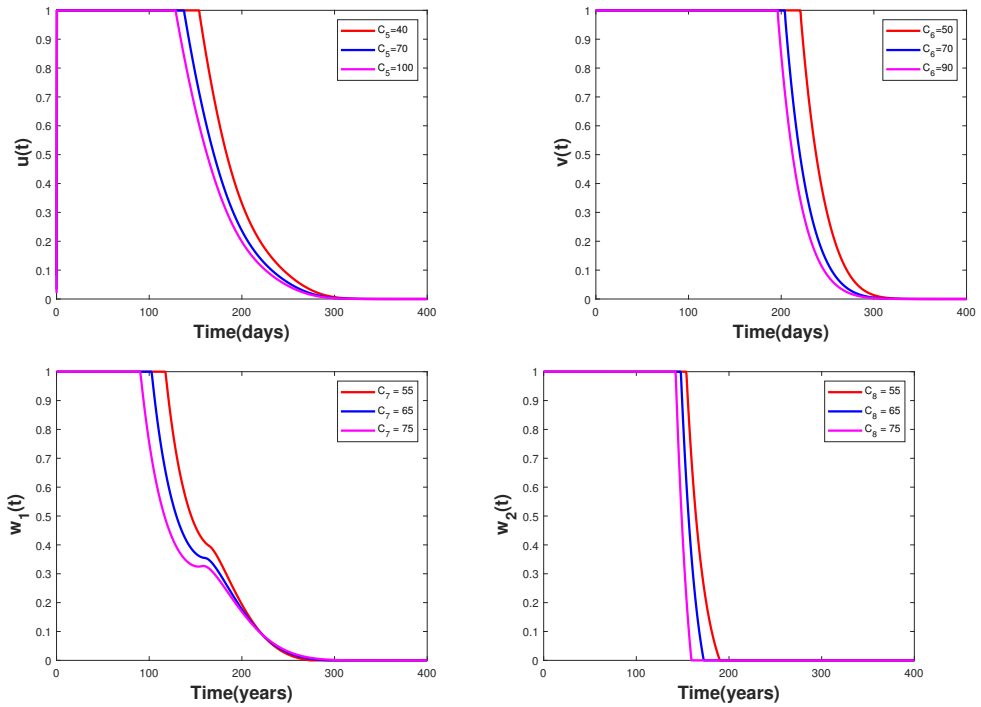

Figure 8: Variations in control variables with respect to relative costs.

6 Conclusion

When precise diagnostic tests or medical facilities were unavailable, compartmental epidemiological models helped us understand how epidemic diseases spread and devise preventative measures. In this paper, SEAIJHRD model was formulated to observe the dissemination dynamics of COVID-19 spread in India. We first established the model's positivity and boundedness, and then, R_0 value was determined to be 1.682. The infection free equilibrium was both LAS and GAS for $R_0 < 1$. By fitting the model to reported COVID-19 data, the infection dissemination rate, hospitalization rates of symptomatic infected and isolated populations were estimated. The sensitive analysis of R_0 determined that both isolation rate (λ_s) and hospitalization rate (η_s) of symptomatic individuals were more effective in reducing R_0. In addition, the proposed model was expanded to an optimal control problem by integrating four controls: 1) awareness programs through media and civil society that the susceptible population do not interact with infected ones 2) vaccination process for susceptible population, and 3) urging the infected population to go into isolation or join hospitals. The combination of four controls had greater impact on reducing the number of infected individuals. Our model concludes that vaccination for susceptible individuals, isolation of the infected population, severe disinfection safeguards using, and social distance maintenance were effective roles in controlling virus spread in a community and may even eradicate the corona virus disease. In future, there will be possible to develop an epidemic model to examine the impact of COVID-19 on HIV/AIDS or TB infected individuals.

References

[1] N. Zhu, D. Zhang, W. Wang, W. Xu, G. Wu, G.F. Gao, W. Tan, China Novel Coronavirus Investigating and Research Team, A Novel Coronavirus from Patients with Pneumonia in China, 2019, N Engl J Med., 382(8), 727-733(2020).

[2] https:// covid19.who.int.

[3] M.L. Danzetta, R. Bruno, F. Sauro, L. Savini, P. Calistri, Rift Valley fever trasmission dynamics described by compartmental models, Prev Vet Med., 134, 197-210(2016).

[4] A. Anirudh, Mathematical modeling and the transmission dynamics in predicting the Covid-19 - What next in combating the pandemic, Infect Dis Model, 5, 366–374(2020).

[5] D.K. Bagal, A. Rath, A. Barua, D. Patnaik, Estimating the parameters of susceptible-infected-recovered model of COVID-19 cases in India during lockdown periods, Chaos, Solitons Fractals, 140, 110154(2020).

[6] N. Anand, A. Sabarinath, S. Geetha, S. Somanath, Predicting the spread of COVID-19 using SIR model augmented to incorporate quarantine and testing, Trans. Indian National Acad. Eng, 5(2), 141–148(2020).

[7] Y. Li, J. Shi, J. Xia, Y. Yuan, L. Gong, X. Yang, H. Gao, C. Wu, Asymptomatic and Symptomatic Patients With Non-severe Coronavirus Disease (COVID-19) Have Similar Clinical Features and Virological Courses: A Retrospective Single Center Study, Frontiers in microbiology, 11, 1570(2020).

[8] E. Armstrong, M. Runge, J. Gerardin, Identifying the measurements required to estimate rates of COVID-19 transmission, infection, and detection, using variational data assimilation, Infect Dis Model, 6, 133-147(2021).

[9] J.T. Wu, K. Leung, G.M. Leung, Nowcasting and forecasting the potential domestic and international spread of the 2019-nCoV outbreak originating in Wuhan, China: a modelling study, Lancet, 395, 689-697(2020).

[10] O. Sharomi, T. Malik , Optimal control in epidemiology, Ann. Oper. Res., 251(1), 55–71(2017).

[11] C.J. Silva, C. Cruz, D.F.M. Torres, A.P. Muñuzuri, W. Abreu, J. Mira, Optimal control of the COVID-19 pandemic: controlled sanitary deconfinement in Portugal, Sci., 11(1), 3451(2021).

[12] J. Mondal, S. Khajanchi, Mathematical modeling and optimal intervention strategies of the COVID-19 outbreak, Nonlinear Dyn, 109(1), 177-202(2022).

[13] N.Fergusonm, Report 9: Impact of non-pharmaceutical interventions (NPIs) to reduce COVID19 mortality and healthcare demand, 2020.

[14] R. Li, S. Pei, B. Chen, Y. Song, T. Zhang, W. Yang, J. Shaman, Substantial undocumented infection facilitates the rapid dissemination of novel coronavirus (SARS-CoV-2), Science, 368, 489–493(2020).

[15] S.A. Lauer, K.H. Grantz, Q. Bi, F.K. Jones, Q. Zheng, N.G. Reich, J. Lessler, The incubation period of coronavirus disease 2019 (COVID-19) from publicly reported confirmed cases: estimation and application, Ann. Internal Med., 172(9), 577–582(2020).

[16] A.B. Gumel, S.Ruan, T. Day, J. Watmough, F. Brauer, P. van den Driessche, J. Wu, B.M. Sahai, Modelling strategies for controlling SARS outbreaks, Proc Biol Sci., 271(1554), 2223-2232(2004).

[17] S.S. Nadim, I. Ghosh, J. Chattopadhyay, Short-term predictions and prevention strategies for COVID-19: A model-based study, Appl. Math Comput., 404, 126251(2021).

[18] K. Sarkar, S. Khajanchi, J.J. Nieto, Modeling and forecasting the COVID-19 pandemic in India, Chaos, Solitons & Fractals, 139, 110049(2020).

[19] S.K. Ghosh, S. Ghosh, A mathematical model for COVID-19 considering waning immunity, vaccination and control measures, 13(1), 3610(2020).

[20] M. Ankamma Rao, A. Venkatesh, SEAIQHRDP mathematical model Analysis for the transmission dynamics of COVID-19 in India, Journal of Computational Analysis & Applications, 31(1), 96-116(2023).

[21] V. Bajiya, S. Bugalia, J. Tripathi, Mathematical modeling of COVID-19: Impact of non-pharmaceutical interventions in India. Chaos, 30, 1063(2020).

[22] S.R. Bandekar, M. Ghosh, Mathematical modeling of COVID-19 in India and Nepal with optimal control and sensitivity analysis. Eur Phys J Plus., 136(10), 1058(2021).

[23] S. Khajanchi, K. Sarkar, J. Mondal, SF. Abdelwahab, Mathematical modeling of the COVID-19 pandemic with intervention strategies, Results Physics, 25, 104285(2021).

[24] Open government data (OGD) platform India or data.gov.in. 2020, data.gov.in/resources/crude-death-rate-india-2011(2020).

[25] O. Diekmann, J.A.P. Heesterbeek, J.A.J. Metz, On the definition and the computation of the basic reproduction ratio R_0 in models for infectious diseases in heterogeneous populations, J. Math. Biol., 28, 365–382(1990).

[26] P.Van den Driessche, J. Watmough, Reproduction numbers and sub-threshold endemic equilibria for compartmental models of disease transmission. Math Biosci, 180, 29-48(2002).

[27] https://data.covid19india.org/

[28] H.S. Rodrigues, M. Teresa, T. Monteiro, F.M. Delfim, Sensitivity Analysis in a Dengue Epidemiological Model, In: Conference Papers in Mathematics, 1-7(2013).

[29] N. Chitnis, J.M. Hyman, J.M. Cushing, Determining important parameters in the spread of malaria through the sensitivity analysis of a mathematical model, Bull Math Biol., 70(5), 1272-1296(2008).

[30] L.S. Pontryagin, Mathematical Theory of Optimal Processes, Routledge, 1987. https://doi.org/10.1201/9780203749319.

[31] J.T. Workman, S. Lenhart, Optimal Control Applied to Biological Models, CRC Press, Boca Raton, 2007(2007).

[32] V.P. Dubey, J. Singh, A.M. Alshehri, S. Dupey, D. kumar, Forecasting the behavior of fractional order Bloch equations appearing in NMR flow via a hybrid computational technique. Chaos, Solitons & Fractals 164, 112691(2022).

[33] V.P. Dubey, J. Singh, A.M. Alshehri, S. Dupey, D. Kumar, Analysis and Fractal Dynamics of Local Fractional Partial Differential Equations Occurring in Physical Sciences. Journal of Computational and Nonlinear Dynamics 18(3), 1-23(2022).

[34] V.P. Dubey, D. Kumar, S. Dupey, A modified computational scheme and convergence analysis for fractional order Hepatitis E virus model, In book: Advanced Numerical Methods for Differential Equations: Applications in Science and Engineering, 279-312 (2021).

[35] V.P. Dubey, J. Singh, A.M. Alshehri, S. Dupey, D. Kumar, Numerical investigation of fractional model of Phytoplankton–Toxic Phytoplankton–Zooplankton system with convergence analysis, Int. J. Biomath. 15(4), 2250006(2022).

[36] V.P. Dubey, D. Kumar, S. Dupey, J. Singh, A computational study of fractional model of atmospheric dynamics of carbon dioxide gas, Chaos, Solitons & Fractals, 142, 110375(2021).

[37] D. Kumar, V.P. Dubey, S. Dupey, J. Singh, A.M. Alshehri, Computational Analysis of Local Fractional Partial Differential Equations in Realm of Fractal Calculus, Chaos, Solitons & Fractals 167, 113009(2023).